www.cadanda.com
Computer-Aided Design AND APPLICATIONS

Five-Axis Tool Positioning of a Toroidal End Mill Tool Near Common Edge Between Two Intersecting Surfaces

Sandeep Kumar Sharma[1], Ravinder Kumar Duvedi[2], Sanjeev Bedi[3] and Stephen Mann[4]

[1]Thapar Institute of Engineering & Technology, India, sksharma@thapar.edu
[2]Thapar Institute of Engineering & Technology, India, rduvedi@thapar.edu
[3]University of Waterloo, Waterloo, ON, Canada, sbedi@uwaterloo.ca
[4]University of Waterloo, Waterloo, ON, Canada, smann@uwaterloo.ca

Corresponding author: Sandeep K. Sharma, sksharma@thapar.edu

Abstract. The transition zone around the common edge of two curved (tensor product) surfaces impacts the performance efficiencies of products like impellers, blisks, turbine blades, etc. The freely accessible region away from the common edge can be machined with a multipoint method. While the transition zone between the two curved surfaces can be machined with Drop Spin Method (DSM) due to Sharma et al. [13]. The tool is first dropped on one of the surfaces near the common edge and is subsequently rotated about the surface normal at first point of contact to achieve the tangency with the second surface. This generates a snugly fitting transition region between the two surfaces, however, the method leaves unwanted material around the common edge between the snugly fit pass and the freely accessible region of the curved surface. In this work, an algorithm that removes this unwanted material is presented. The proposed concept is validated on a sample of two intersecting surfaces, using Maple graphics simulations, a custom open GL based five-axis NC machining simulator and by performing actual machining on DMU 80-P Hi-Dyn tilt rotary simultaneous five-axis CNC machining center. First the two surfaces were machined using Drop and Tilt (DTM) algorithm [5] followed by the snugly fit pass, using DSM algorithm. The algorithm was then used to produce a set of toolpaths for 5-axis clean-up machining around the region of common edge. The algorithm was tested on the sample part.

Keywords: Multipoint five-axis machining, toroidal end mill, tensor product surfaces, drop spin method DSM
DOI: https://doi.org/10.14733/cadaps.2020.699-715

1 INTRODUCTION

5-axis machining offers the potential benefit of achieving higher machining efficiencies particularly in machining sculptured/complex surfaces as seen predominantly in forming dies, aerodynamic surfaces, turbine blades, etc. The use of complex surfaced components has proven beneficial in

© 2020 CAD Solutions, LLC, http://www.cad-journal.net

enhancing process and product efficiencies in many engineering applications. A challenge to 5-axis machining is the radiused transformation between two curved surfaces. Such radiused transition surfaces exist in turbine blade assemblies, blisks, impellers, etc. and effect the performance efficiencies of these devices. From an engineering perspective smooth transition is preferred over a sharp corner. The machining of such transition surfaces is discussed in this paper.

The intersection of two surfaces can occur in an open area with unimpeded access or in a confined area with potential for interference between part and the tool. For the development of a strategy to machine a radiused transition area, this paper will only deal with easily accessed surfaces. The complex subject of interference avoidance will be addressed in the future.

Amongst the known methods of 5-axis machining of curved surfaces, such as, Multi-Point Method (MPM) [15-17], Principal Axis Method (PAM) [11], etc., the Drop-Tilt Method (DTM) [5] can be used to determine a single toolpath across the two joining surfaces. Alternatively, the two surfaces can be machined with two independent tool paths (a method adopted in this work). In either method, as the tool approaches the common edge, the tool lifts to avoid gouging the other surface. This lift results in unmachined material being left on either side of the common edge. Following on the lines of DTM, Sharma et. al. [13] developed a strategy called the Drop Spin Method (DSM), in which the highest curvature portion of the tool's cutting surface is fit into the corner along the common edge by first dropping the tool onto one of the two surfaces and subsequently spinning the tool about the surface normal at the first point of contact, until an orientation that gives a smooth but high curvature transition between the two surfaces is found. As such transition tool positions are found at many points along the common edge, a toolpath that results in a smooth high curvature transition surface, called the snuggly fit pass, can be obtained as discussed by Sharma et al. [13]. The snuggly fit pass, however, does not remove all the unwanted material near the common edge. The removal of this unwanted material around the snuggly fit pass is the goal of this paper.

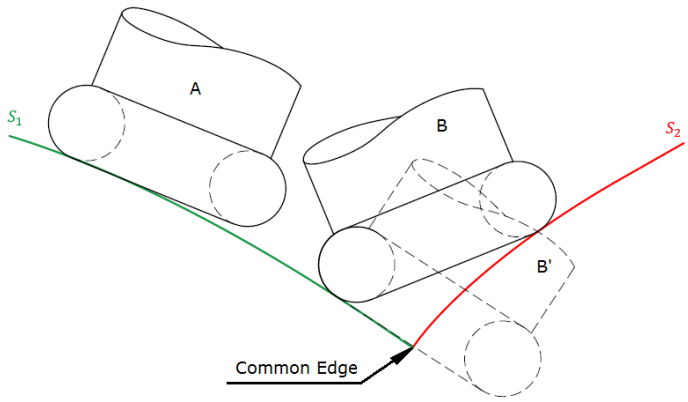

Figure 1: A toroidal end mill in moving across the common edge of two intersecting surfaces using the DTM algorithm [5]. The tool position marked as A is a multipoint tool position on triangulated surface S_1; the tool position marked B' is the expected five-axis tool positioning on surface S_1 in case surface S_2 is not present. The tool is lifted as shown by position marked B when surface S_2 is present.

In this work, the DTM is used to create five-axis machining passes to machine two curved surfaces with a common edge. As the tool passes from one surface to the other surface over the common edge, the tool lifts to avoid gouging the other surface. The tendency of this lift is the function of the tool geometry specifically the values of R_o and R_i as well as the curvature of surfaces around the common edge. In the sketch given in Figure 1, S_1 and S_2 represent the two surfaces. Tool position A represents the DTM tool position away from the common edge. B represents the tool position near

© 2020 CAD Solutions, LLC, http://www.cad-journal.net

the common edge. In absence of S_2 the tool position would be B', but because of the presence of S_2 the tool is lifted to position B leaving uncut material under it. To address this issue, Sharma et al. [13] identified a tool footprint zone called "spin-zone" which effects the tool positioning over common edge region for a given pair of intersecting surfaces (described later).

DSM technique by Sharma et al. [13] helps find a snugly-fit five-axis tool orientation at a given footprint point along a common edge within the spin-zone where the tool touches tangentially on one point each on the two adjoining surfaces and the two points lie on the neighboring pseudo-inserts of the toroidal tool. This snugly-fit DSM machining pass best fits the given toroidal tool over the common edge with formation of a radiused corner between surfaces S_1 and S_2. The curvature of the snugly fit surface can be changed by changing the insert radius R_i. The curvatures of the two surfaces around the common edge region still has unmachined material. Additional multipoint machining passes are required to remove such left over material along the two sides of the snugly machined radiused corner on the common edge. The work presented in this paper is focused in determining such additional multipoint machining passes.

2 BACKGROUND

Multipoint five-axis machining of complex engineering surfaces with a toroidal end mill offers several advantages compared to machining using a flat or a ball end milling cutters [1-13], [15-18]. The multipoint tool positioning using toroidal end milling cutter has evolved over last two decades. The key focus in multipoint machining is to engage the toroidal cutter for five-axis machining while ensuring the tangency at more than one point of contact between tool and the machined surface. The method ensures gouge free machining and better surface finish. Moreover, the multi-tangency tool positioning in five-axis machining results in wider machining strips with errors less than the user specified tolerances, thereby enabling the machining of the surface to be accomplished in lesser number of machining passes.

Significant amount of work has been accomplished to enable the use of toroidal end milling tool for multipoint five-axis machining [10], [12]. Warkentin et al. [15] compared the early developments in multipoint tool positioning for surface machining using a toroidal end milling tool for curved surfaces. The available methods of surface machining using five-axis multipoint tool positioning using a toroidal end mill, take the surface data in the analytical or parametric form as investigated in Principle Axis Method by Rao et al. [11], Principal Curvature Alignment Technique by Bedi et al. [1], Intersection Approach and multipoint methods by Warkentin et al. [16-17] and Arc intersect Method by Gray et al. [7] for machining of parametric surfaces or when the surfaces are taken in the form of triangulated facets as in the case of Rolling Ball Method by Gray et al. [8] and Drop and Tilt Method by Duvedi et al. [5]. The most recent development for Drop and Tilt method (DTM) by Duvedi et al. [4], [6] and Drop Tilt and Spin method (DSTM) by Sharma et al. [12] solved for gouge-free multi-tangency multipoint five-axis tool positioning directly for tensor product Bézier surfaces to make the technique more versatile for industrial use. The direct method is computationally more accurate as well as efficient.

One interesting case is the five-axis machining of the narrow region of two intersecting parametric surfaces as found in the case of machining the region of the hub and the blade intersection zone for a turbine blade. Though such a narrow region can be machined using a ball end mill cutter, a multipoint machining using a toroidal end mill can help achieve better machining productivity as well as surface finish and tool life.

Derived from "Drop the Tool Concept" of toroidal tool positioning by Duvedi et al. [5], the DSM [13], the DTM [4], [6] and the DSTM [12] methods compute the five-axis tool positioning in two stages. In the first stage, the tool is dropped on a given surface to determine the first point of tangency between tool and the surface. In the second stage, the tool is rotated about the spin-axis direction given by the surface normal at first point of contact or the pseudo-insert axis to find the second point of tangency between the tool and the surface. Table 1 compares the DSM, DTM and

© 2020 CAD Solutions, LLC, http://www.cad-journal.net

DSTM methods. The contribution of this paper is to extend DSM for 5-axis tool positioning to clean the uncut material in the common intersection region of the two surfaces.

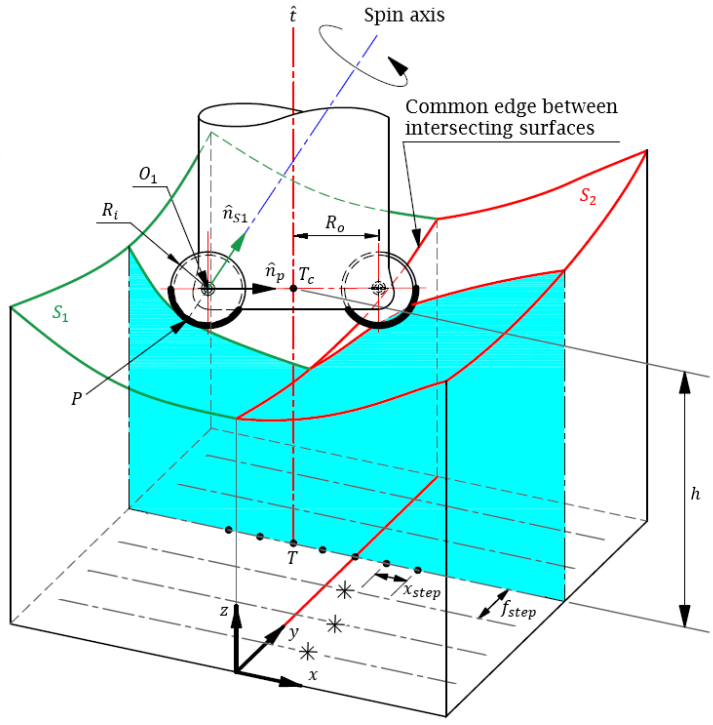

Figure 2: The geometric definition of a toroidal end mill tool and the definition of the toolpath footprint points determined to implement DSM tool positioning.

Method Characteristics	**DTM**	**DSTM**	**DSM**
Tool position on two tensor product surfaces simultaneously	X	X	√
Tool position in the intersection region of two intersecting surfaces	X	X	√
Gouge free	√	√	√
Control of spacing between contact points	X	√	X
Drop tool along the tool axis	√	√	√
Tilt tool along the pseudo-insert axis	√	√	X
Spin tool along the surface normal through first point of contact	X	√	√

Table 1: Comparison of different methods for tool positioning.

3 CONCEPT OF DROP AND SPIN METHOD

The five-axis tool positioning algorithm presented in this paper is based on DSM [13] approach and employs a toroidal tool. The geometry of a toroidal cutter can be thought of as a solid of revolution generated by sweeping a circular insert of radius R_i about the center of torus wherein the center of the insert is located at a distance R_o from the center of torus. The circle of insert of radius R_i is also called the *pseudo-insert circle*, and the offset distance between the centers of torus to the center of

© 2020 CAD Solutions, LLC, http://www.cad-journal.net

pseudo-insert circle, given by R_o, is called the major radius of torus. The Figure 2 shows the geometry of a general toroidal end mill tool and the axis of the toroidal tool is shown by direction vector $\hat{t}$.

The key deliverable of the DSM five-axis tool positioning algorithm is a pair of gouge free contact points on each of the two intersecting surfaces around the common edge of interest for each tool position. To determine the complete five-axis tool positioning data for machining the region of the common edge between the two intersecting tensor product surfaces, a series of tool-drop footprint locations need to be identified on the xy-plane, referred to as the *footprint plane*. In the present work, we have used tool footprint points, given by T, as shown in Figure 2. The tool footprint points are located on the reference lines drawn normal to the projection of common edge on the xy −plane and are f_{step} apart. To determine the footprint points on the reference lines, equi-spaced points with a separation of x_{step} are considered (shown as dots on the reference lines in Figure 2). The final location of the footprint point T (shown as asterisk) at any given reference line is determined depending on the desirable gap between the two contact points as described in section 4.

The extension of DSM algorithm developed in this work uses two stepped procedure to determine the two points of contact with the two intersecting surfaces. In the first step, named "Tool Drop" the toroidal tool is dropped on one of the surfaces to compute the point of tangency between the tool and the surface. This surface is termed as "Tool-Drop Surface" and the tool contact point is referred as first point of contact. In the second step, called "Tool Spin", the tool is rotated about the surface normal through the first point of contact to determine a spin angle so that the tool touches the second surface tangentially. The location of the point of tangency of tool on the second surface is referred to as the second point of contact. The procedure to determine the two points of contacts and five-axis tool orientation is described below:

Step-I (Tool Drop):

In this step, the toroidal tool is dropped on one of the intersecting surfaces (say S_1), with its axis $\hat{t}$ being vertical and passing through a footprint location T as shown in Figure 3(a). The tool makes a tangential contact with surface S_1 at point $P = S_1(u_1, v_1)$ which is determined from the following equation:

$$S_1(u_1, v_1) + R_i\hat{n}_{S1} + R_o\,\hat{n}_p - \hat{t}\mathrm{h} - T = 0 \tag{3.1}$$

where, $\hat{n}_{S1}$, $\hat{n}_p$ and h are the surface normal to surface S_1 through the first point of contact P, the direction vector normal to tool-axis $\hat{t}$ and the height of the tool center T_c above footprint point T respectively and are determined as given below:

$$\hat{n}_{S1}(u_1, v_1) = \frac{\frac{\partial S_1(u_1,v_1)}{\partial u_1} \times \frac{\partial S_1(u_1,v_1)}{\partial v_1}}{\left\| \frac{\partial S_1(u_1,v_1)}{\partial u_1} \times \frac{\partial S_1(u_1,v_1)}{\partial v_1} \right\|}$$

$$\hat{n}_p = \frac{\hat{n}_{S1} - \{\hat{n}_{S1}.\,\hat{t}\}\,\hat{t}}{\|\hat{n}_{S1} - \{\hat{n}_{S1}.\,\hat{t}\}\,\hat{t}\|}$$

$$T_c = T + \hat{t}h$$

The point P is determined by solving Equation (3.1) for (u_1, v_1, h). The center of the pseudo-insert circle O_1, for the pseudo-insert at point P is given as:

$$O_1 = P + R_i\hat{n}_{S1} \tag{3.2}$$

A toroidal tool with its center at T_c can be defined using a coordinate frame $\{\hat{\imath}_0, \hat{\jmath}_0, \hat{k}_0\}$, whereas this frame is located at the center of the pseudo-insert circle O_1 as shown in Figure 3(a). The frame $\{\hat{\imath}_0, \hat{\jmath}_0, \hat{k}_0\}$ is given as:

$$\{\hat{\imath}_0, \hat{\jmath}_0, \hat{k}_0\} = \{\hat{\jmath}_0 \times \hat{k}_0\,, \hat{n}_p, \hat{t}\,\}$$

Step-II (Tool Spin):

As a result of the first stage, the dropped tool while touching the first surface S_1 tangentially, may or may not gouge with the second surface S_2. The gouging of the toroidal tool with the second surface depends on the location of the footprint point T in the first stage.

© 2020 CAD Solutions, LLC, http://www.cad-journal.net

In this stage, the toroidal tool is rotated about surface normal $\hat{n}_{S1}$ by an angle α until the rotated tool is made to touch the second surface S_2 tangentially at point $Q = S_2(u_2, v_2)$. The direction vector $\hat{n}_{S1}$ and the point Q are referred in this work as the spin-axis and the second point of contact respectively. The tool rotation about the spin-axis ensures that the contact between tool and surface S_1 at P is maintained.

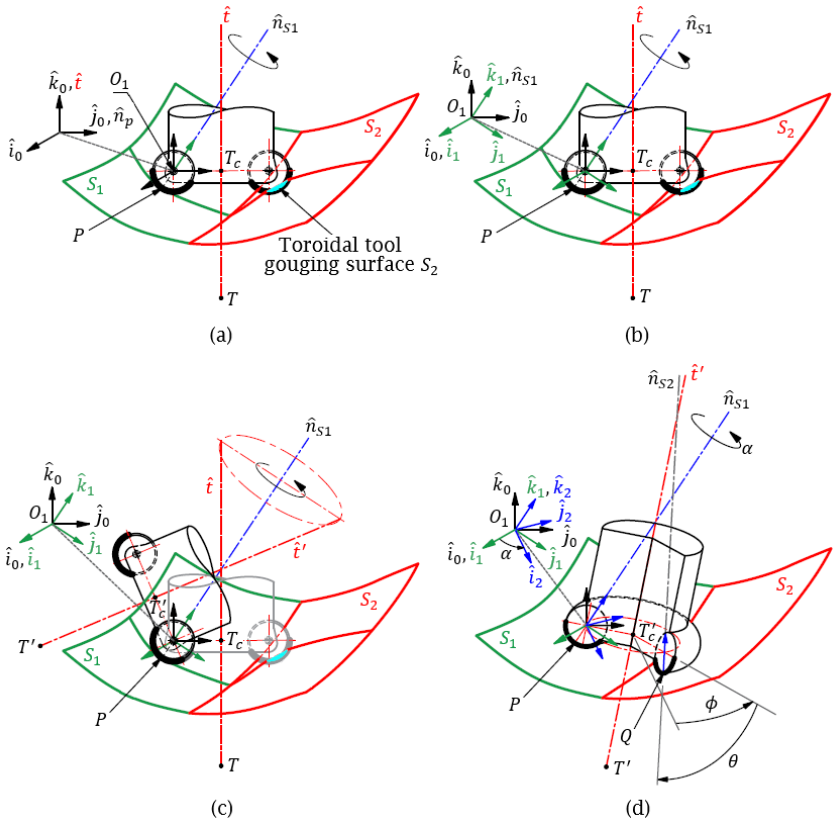

Figure 3: Definition of geometric parameters used in DSM method: (a) Step-1: determining the first point of contact P between surface S_1 and the vertical dropped toroidal tool at suitable footprint location T, (b) Step-2: determining the spin-axis for tool rotation, (c) concept of rotating toroidal tool about spin-axis, (d) Step-3: determining the spin angle α that enables a second point of contact Q of toroidal tool on surface S_2 while tool also retains its tangency to S_1 at P.

To determine the second point of contact, another coordinate frame $\{\hat{i}_1, \hat{j}_1, \hat{k}_1\}$, referred to as the Tool-Spin frame (see Figure 3 (b)), is defined with its origin at $O_1$and is given as:

$$\{\hat{i}_1, \hat{j}_1, \hat{k}_1\} = \{\hat{i}_0, \hat{n}_{S1} \times \hat{i}_1, \hat{n}_{S1}\}$$

While the tool is rotated about spin-axis, the tool-axis $\hat{t}$ rotates to generate a cone as shown in Figure 3(c). Each generatrix of this cone swept by tool-axis can be a possible five-axis tool orientation. Two of these rotated tool-axis orientations are unique in the sense that they result in tangency of the tool at two different locations for the second points of contact Q (say Q_1 or Q_2) with the second surface S_2. This leads to two possibilities for the spin solutions for the second point of

© 2020 CAD Solutions, LLC, http://www.cad-journal.net

contact at a given first point of contact P. Thus, we have two possible solutions for the five-axis multipoint tool positioning given by the two tangential set of contact points $\{P, Q_1\}$ and $\{P, Q_2\}$.

After the tool has been rotated about spin axis, the new orientation of the local coordinate frame $\{\hat{\imath}_1, \hat{\jmath}_1, \hat{k}_1\}$ at point O_1 is given by frame $\{\hat{\imath}_2, \hat{\jmath}_2, \hat{k}_2\}$. The direction vectors of frame $\{\hat{\imath}_2, \hat{\jmath}_2, \hat{k}_2\}$ are shown in Figure 3(d) and are defined as:

$$\{\hat{\imath}_2, \hat{\jmath}_2, \hat{k}_2\} = \{cos\alpha\ \hat{\imath}_1 + sin\alpha\ \hat{\jmath}_1, -sin\alpha\ \hat{\imath}_1 + cos\alpha\ \hat{\jmath}_1,\ \hat{k}_1\}$$

The post spin orientation and the position of the toroidal tool are mapped back to the initial coordinate frame $\{\hat{\imath}_0, \hat{\jmath}_0,\ \hat{k}_0\}$ from $\{\hat{\imath}_2, \hat{\jmath}_2,\ \hat{k}_2\}$ by pre-multiplying with a transformation matrix R_{DSM},which is defined as

$$R_{DSM} = R_0^1\ R_1^2\ R_0^{1^T} \tag{3.3}$$

where R_a^b is the rotation matrix representing the mapping from coordinate frame $\{b\} = \{\hat{\imath}_b, \hat{\jmath}_b, \hat{k}_b\}$ to frame $\{a\} = \{\hat{\imath}_a, \hat{\jmath}_a, \hat{k}_a\}$ and is given as

$$R_a^b = \begin{bmatrix} \hat{\imath}_a \cdot \hat{\imath}_b & \hat{\imath}_a \cdot \hat{\jmath}_b & \hat{\imath}_a \cdot \hat{k}_b \\ \hat{\jmath}_a \cdot \hat{\imath}_b & \hat{\jmath}_a \cdot \hat{\jmath}_b & \hat{\jmath}_a \cdot \hat{k}_b \\ \hat{k}_a \cdot \hat{\imath}_b & \hat{k}_a \cdot \hat{\jmath}_b & \hat{k}_a \cdot \hat{k}_b \end{bmatrix}$$

Further, the definition of the rotated toroidal tool with respect to a global Cartesian coordinate frame $\{x, y, z\}$ in its post spin configuration is represented by T'_{tool} and is given by:

$$T'_{tool} = T'_c + R_{DSM}\ T_{tool}$$

where T'_c is the center of the toroidal tool in post spin configuration defined in frame $\{x, y, z\}$ and is given by

$$T'_c = O_1 + R_{DSM}\ T_c$$

where T_c is the center of toroidal tool with respect to coordinate frame $\{\hat{\imath}_0, \hat{\jmath}_0, \hat{k}_0\}$ at O_1 and is defined as

$$T_c = [0, R_o, 0]^T$$

and T_{tool} is the definition of toroidal tool with respect to coordinate frame $\{\hat{\imath}_0, \hat{\jmath}_0, \hat{k}_0\}$ centered about T_c and is defined as

$$T_{tool} = [(R_o + R_i cos\theta)cos\phi, \quad (R_o + R_i cos\theta)sin\phi, \quad R_i sin\theta]^T$$

The variable θ and ϕ are the angles used to model the toroidal tool in its initial frame $\{\hat{\imath}_0, \hat{\jmath}_0,\ \hat{k}_0\}$ and are shown in Figure 3(d).

Similarly, in the post spin configuration, the new orientation of the tool-axis $\hat{t}'$ and the definition of the major circle of the toroidal tool C'_{tool} having its center T'_c in $\{x, y, z\}$ are given as:

$$\hat{t}' = R_{DSM}\ \hat{t}_0$$

$$Cir'_{tool} = T'_c + R_{DSM}\ Cir_{tool}$$

where $\hat{t}_0 = [0, 0, 1]^T$ and $Cir_{tool} = [R_o cos\phi, \quad R_o sin\phi, \quad 0]^T$

For the rotated toroidal tool, to compute the point of contact with the surface S_2 at $Q = S_2(u_2, v_2)$, the locus of the center of the pseudo-insert through point Q must lie on the major circle of the rotated toroidal tool Cir'_{tool}. Thus the following equation is solved to obtain Q and the spin angle α,

$$S_2\,(u_2, v_2) + R_i \hat{n}_{S2} - Cir'_{tool} = 0 \tag{3.4}$$

where $\hat{n}_{S2}$ is the surface normal at second point contact $Q = S_2\,(u_2, v_2)$.

Equation (3.4) has three component equations with four unknowns, namely u_2, v_2, α and ϕ. To solve Equation (3.4), another constraint is used, which is

$$\{T'_c - S_2\,(u_2, v_2)\} \cdot \{\hat{t}' \times \hat{n}_{S2}\} = 0 \tag{3.5}$$

Equation (3.5) exploits the fact that the shortest distance between the surface normal at the second point of contact $S_2\,(u_2, v_2)$ and the rotated tool-axis orientation $\hat{t}'$ is zero.

Equations (3.4) and (3.5) are simultaneously solved to obtain (u_2, v_2, α, ϕ) which are further used to compute point Q, surface normal $\hat{n}_{S2}$ and direction vectors $\{\hat{\imath}_2, \hat{\jmath}_2, \hat{k}_2\}$.

© 2020 CAD Solutions, LLC, http://www.cad-journal.net

The procedure given above yield two different solutions for the second point of contact Q, say Q_1 and Q_2, which are obtained as a result of two solutions obtained from Maple symbolic solver for the spin angle α for the given second surface S_2.

Alternatively, the toroidal tool can be dropped on surface S_2 and rotated about the spin-axis to find second point of contact on surface S_1.

3.1 Identification of Feasible Spin Zone

The location of the tool-drop footprint T is critical parameter in DSM. At a given footprint location T, the dropped tool may find gouge free tangency at points P and Q simultaneously with one point on each of the intersecting surfaces as shown in Figure 4(a). In this case there is no scope for the tool to spin, since tool is already touching both the surfaces tangentially. Distance between the two contact points, P and Q, is maximum for this case.

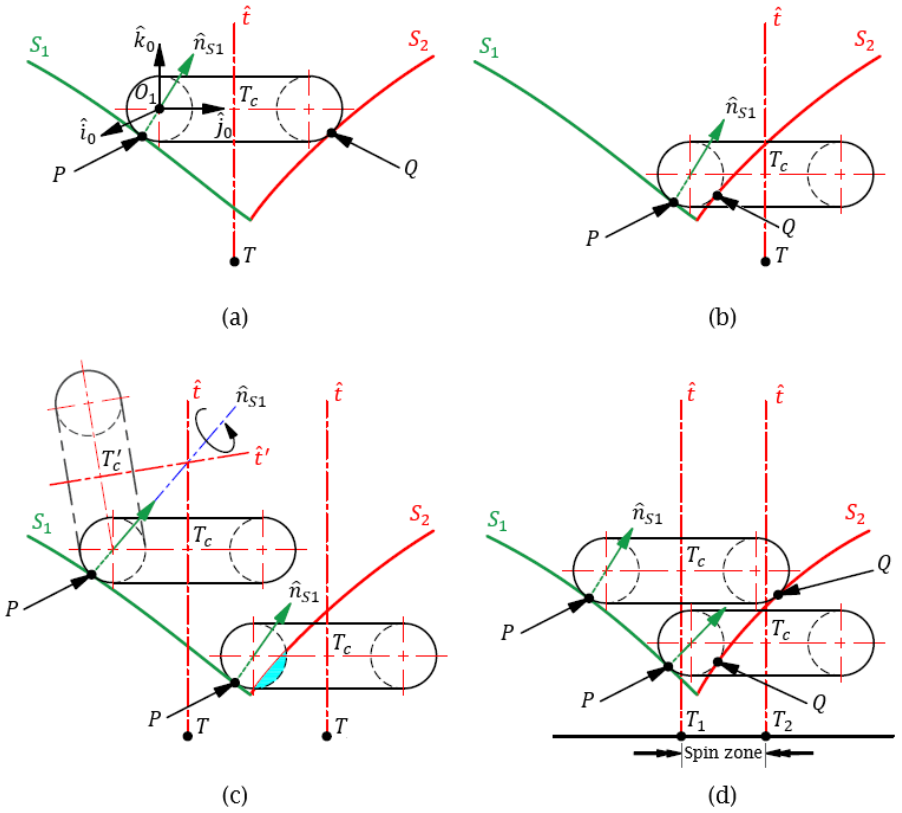

Figure 4: Footprint locations defining the boundary of spin-zone at a given location on the common edge of intersection between set of two tensor product surfaces S_1 and S_2 : (a) footprint location at which the vertically dropped toroidal tool is tangent to both the surfaces, (b) footprint location at which a unique single pseudo-insert touches both the surfaces. Any tool drop footprint location towards right hand side of this footprint location will always gouge second surface S_2 for complete range of spin angle $(-\pi \leq \alpha \leq \pi)$, (c) infeasible footprint locations for DSM method, (d) limiting toolpath footprint locations for the spin-zone.

© 2020 CAD Solutions, LLC, http://www.cad-journal.net

On the other extreme, there can be a footprint location where the dropped tool may be simultaneously tangent with both the intersecting surfaces, while the two points of contact P and Q lie on the same "*pseudo insert circle*" as shown in Figure 4(b). In other words, this small circle of the toroidal tool is tangent to both the intersecting surfaces at P and Q. In this case, when the tool is rotated about spin-axis $\hat{n}_{S1}$, there is a unique spin angle for which the tool just touches surfaces S_1 and S_2 without gouging. This footprint location ensures that the tool fits snugly into the region near the common edge and the two contact points are as close as possible to the common edge. This results in the maximum possible material removal in the common edge zone.

The above stated two limiting footprint locations ensure that the rotated tool is tangent to both intersecting surfaces. However, in Figure 4(a), if the footprint location T is shifted further towards left hand side towards tool-drop surface S_1, the dropped tool finds no intersection with the second surface S_2. In such a situation, the rotated tool will not be able to contact the second surface S_2, as shown in Figure 4(c).

On the other hand, as shown in Figure 4(b), if the footprint location T is shifted further to right hand side towards the surface S_2, the pseudo-insert circle through first point of contact P intersects with the surface S_2 as shown with Turquoise shaded zone in Figure 4(c). Such tool footprint locations are avoided in this work as no spin-angle value will be able to provide the gouge free tool orientation. So the feasible tool-drop positions that can result in gouge free tangency between the rotated tool and two intersecting surface is limited between two footprint locations as shown in Figure 4(a) and 4(b). This range bounded between limiting footprint locations T_1 and T_2, is termed as the *Spin-Zone* and is shown in Figure 4(d). This method will yield a number of valid multipoint tool positions when the footprint locations lie within the *Spin-Zone*.

At any location along common edge, the *Spin-Zone* is not unique as it depends on the tool-drop surface. Another second *Spin-Zone* exists on the left side of the common edges shown in Figure 4(d), in case tool is dropped on surface S_2. This *Spin-Zone* is created as the tool approaches the common edge from right to left direction. In such situation, T_1 and T_2 will lie on right and left side of the common edge respectively.

The lifting of the tool to avoid intersection with second surface begins to take place at the start of the *Spin-Zone* and culminates at the snugly fit tool position as shown in Figure 4(b). Many viable tool orientations exist between these two extremes. *Spin-Zone*, defined by such limiting tool-drop positions T_1 and T_2, is determined at various y-axis locations along the common edge.

3.2 Determining the Spin Zone Limits

For a given size of toroidal tool, the *Spin-zone* footprint limits T_1 and T_2, depend on the shape of the 3D curve representing the common edge. The procedure begins with the dropping the tool on a surface and then rotating it about the spin-axis. The spin solution may or may not exist. If spin solution does not exist, then the tool-drop footprint position is incremented, pushing it towards T_2 through x_{step} until a feasible spin solution is available. This procedure is repeated until two consecutive tool-drop positions are available for which the spin solution is alternate, which means, one tool drop does not have spin solution and the next one has. Bisection method with a specified precision is applied on these two consecutive tool drop positions to determine the location of T_1.

Similarly, when the spin solution exists, the rotated tool position is tested for gouging [6]. If the gouge check is positive, the tool drop position is pushed towards T_1 through x_{step}. Otherwise the tool drop position is incremented in the opposite direction. This procedure continues until two consecutive tool drop positions are determined for which the gouge check results are opposite. The location of T_2 is determined by applying the bisection method with a specified precision.

© 2020 CAD Solutions, LLC, http://www.cad-journal.net

3.3 The Proposed Strategy

The snugly fit pass creates a radiused transition surface, but it is unable to completely remove the excess undesired material adjacent to the radiused transition generated over the common edge. To remove this material, the *Spin-Zone*, is divided into a number of tool-drop locations and the DSM tool orientations are determined. This step is repeated at many points along the common edge. By connecting the appropriate DSM tool orientations, toolpaths along the common edge are created. As the tool traverses these tool paths, it touches both the surfaces on either side of the common edge. The contact points on the two surface may not be evenly spread across the region around the common edge. To ensure that all excess material in common edge region is removed, similar tool paths are also generated in the second *Spin-Zone* due to surface S_2.

4 RESULTS & DISCUSSIONS

We tested the above concept on two separate sets of intersecting bi-quadratic Bézier surfaces [13]. Table 2 shows the control points of the pairs of concave and convex intersecting surfaces.

(a) Control points for intersecting Bi-Quadratic Concave surfaces S_1 and S_2		
$S_{1_{0,0}}$ = (0.0, 0.0, 4.0)	$S_{1_{0,1}}$ = (0.0, 25.0, 0.0)	$S_{1_{0,2}}$= (0.0, 50.0, 4.0)
$S_{1_{1,0}}$= (-25.0, 0.0, 8.0)	$S_{1_{1,1}}$ = (-25.0, 25.0, 6.0)	$S_{1_{1,2}}$= (-25.0, 50.0, 10.0)
$S_{1_{2,0}}$= (-50.0, 0.0, 16.0)	$S_{1_{2,1}}$= (-50.0, 25.0, 12.0)	$S_{1_{2,2}}$ = (-50.0, 50.0, 16.0)
$S_{2_{0,0}}$= (0.0, 0.0, 4.0)	$S_{2_{0,1}}$= (0.0, 25.0, 0.0)	$S_{2_{0,2}}$= (0.0, 50.0, 4.0)
$S_{2_{1,0}}$= (25.0, 0.0, 10.0)	$S_{2_{1,1}}$= (25.0, 25.0, 6.0)	$S_{2_{1,2}}$= (25.0, 50.0, 16.0)
$S_{2_{2,0}}$ = (50.0, 0.0, 20.0)	$S_{2_{2,1}}$ = (50.0, 25.0, 14.0)	$S_{2_{2,2}}$ = (50.0, 50.0, 18.0)
(b) Control points for intersecting Bi-Quadratic Convex surfaces S_1 and S_2		
$S_{1_{0,0}}$ = (0.0, 0.0, 2.0)	$S_{1_{0,1}}$ = (0.0, 25.0, 5.0)	$S_{1_{0,2}}$ = (0.0, 50.0, 2.0)
$S_{1_{1,0}}$ = (-25.0, 0.0, 9.0)	$S_{1_{1,1}}$ = (-25.0, 25.0, 15.0)	$S_{1_{1,2}}$ = (-25.0, 50.0, 8.0)
$S_{1_{2,0}}$ = (-50.0, 0.0, 10.0)	$S_{1_{2,1}}$= (-50.0, 25.0, 18.0)	$S_{1_{2,2}}$= (-50.0, 50.0, 12.0)
$S_{2_{0,0}}$ = (0.0, 0.0, 2.0)	$S_{2_{1,1}}$ = (0.0, 25.0, 5.0)	$S_{2_{1,2}}$ = (0.0, 50.0, 2.0)
$S_{2_{1,0}}$= (25.0, 0.0, 4.0)	$S_{2_{1,1}}$ = (25.0, 25.0, 16.0)	$S_{2_{1,2}}$ = (25.0, 50.0, 7.0)
$S_{2_{2,0}}$ = (50.0, 0.0, 12.0)	$S_{2_{2,1}}$= (50.0, 25.0, 20.0)	$S_{2_{2,2}}$ = (50.0, 50.0, 13.0)

Table 2: Control points for pair of intersecting surfaces: (a) Concave surfaces, (b) Convex surfaces.

Figure 7 and 8 show the plots of two pairs of surfaces on which the extended DSM concept discussed in section 3 is implemented in Maple symbolic solver. The tool path for finish machining along the common edge was computed at reference lines which are $f_{step} = 2.5$ mm apart. The *Spin-Zone* limits, T_1 and T_2, were evaluated at all such locations using $x_{step} = 1.0\ mm$. Bisection method is employed to evaluate T_1 and T_2 within a tolerance of $\varepsilon_B = 0.0001\ mm$. A gouge check tolerance of $\varepsilon_G = 0.0001\ mm$ is used to ensure gouge free tangency between the tool and the surfaces.

The algorithm given in section 3 computes two locations of second points of contact, Q_1 and Q_2, for the rotated tool for each tool drop footprint location within spin-zone. However, for the snugly fit machining pass, as shown in Figure 4 (b), these two locations are too close to be differentiated with respect to positioning accuracy of most of the five-axis machining centers. The tool orientations corresponding to these two independent second points of contact are also same. Further, for snuggly

© 2020 CAD Solutions, LLC, http://www.cad-journal.net

fit machining pass, the set of first and second points of contact on the two surfaces are invariant with respect to the drop surface. This is due to the fact that for any position along the common edge, there is a unique snugly fit geometric orientation of the pseudo-insert circle irrespective of the tool-drop surface.

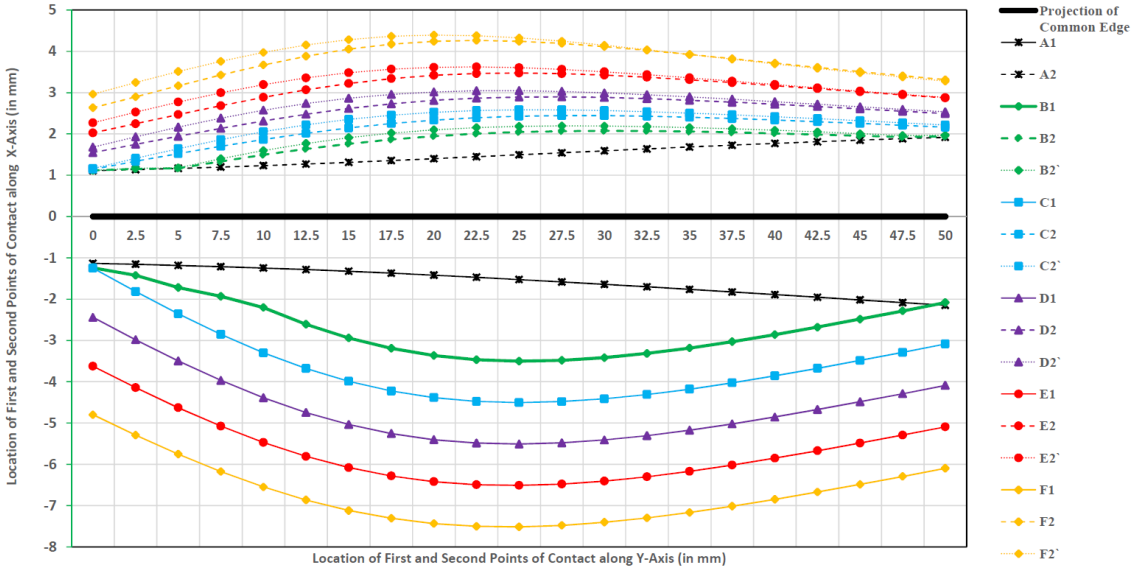

(a)

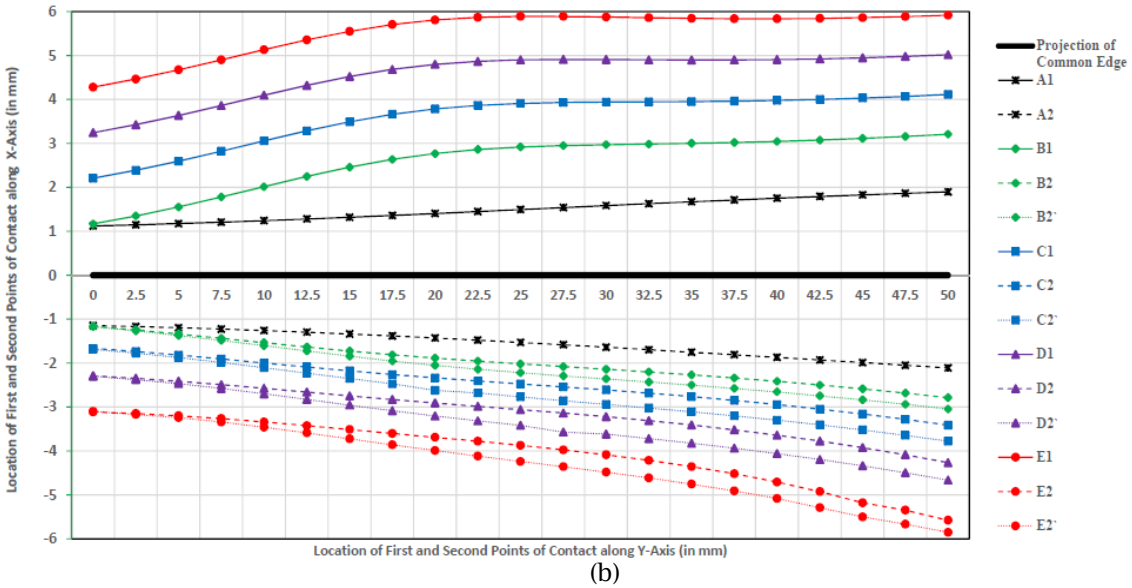

(b)

Figure 5: Trajectories of first and second points of contact for multi-pass finish machining of common edge region between two intersecting Bi-quadratic concave Bézier surfaces: (a) First point of contact on S_1 and second point of contact on S_2, (b) First point of contact on S_2 and second point of contact on S_1.

© 2020 CAD Solutions, LLC, http://www.cad-journal.net

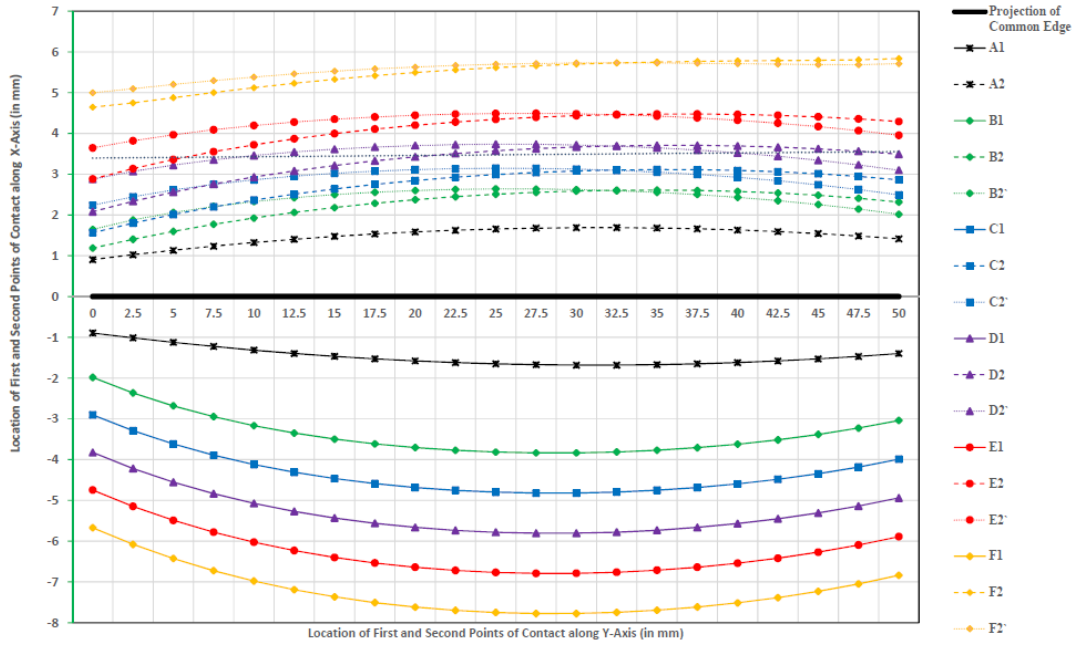

(a)

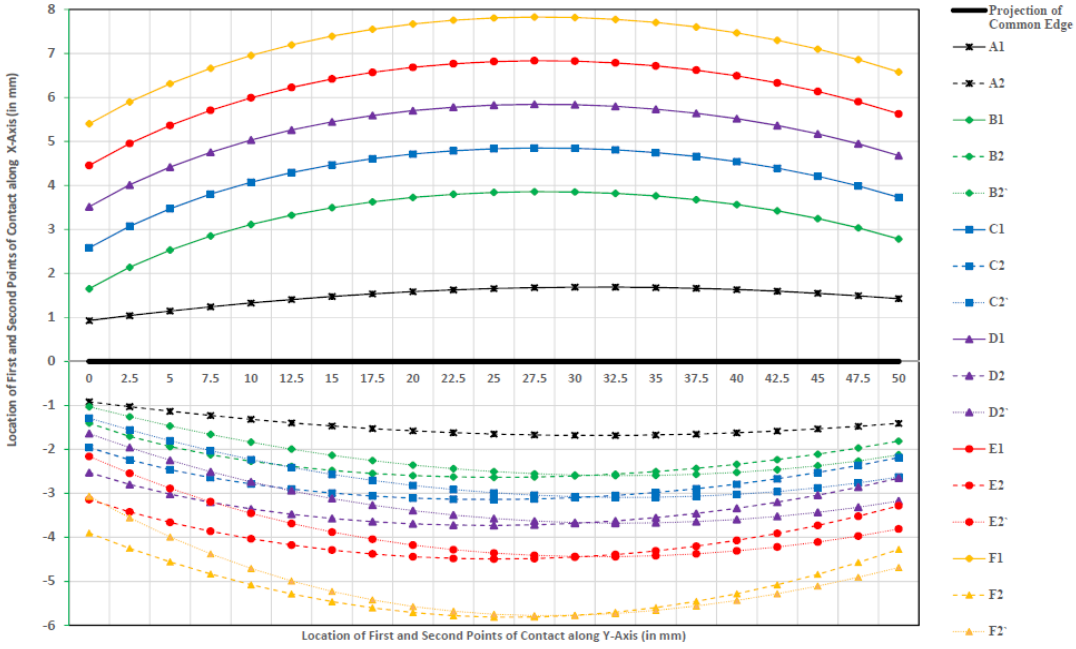

(b)

Figure 6: Trajectories of first and second points of contact for multi-pass finish machining of common edge region between two intersecting Bi-quadratic convex Bézier surfaces: (a) First point of contact

© 2020 CAD Solutions, LLC, http://www.cad-journal.net

on S_1 and second point of contact on S_2, (b) First point of contact on S_2 and second point of contact on S_1.
As the tool is dropped away from the tool footprint location, which yielded the snugly fit pass, two distinct second points of contact Q_1, and Q_2 are obtained. There are two possible tool-axis orientations corresponding to Q_1, and Q_2 and these tool orientations correspond to possible direction of rotation of tool about spin-axis. One of these two available tool orientations may be selected depending upon whether leading or trailing edge of the rotated tool is to be employed for material removal. A tool-path is generated by selecting consistent tool orientations so as to have smooth tool motion during clean-up machining in the region of the common edge.

Figure 5 shows the top view of the common edge marked in black at $X = 0$ and the snuggly fit pass is labeled as **A**. In Figure 5(a) the first point of contact lies on surface S_1 and the second point of contact lies on surface S_2. The space beyond the snuggly contact points is the location of the unwanted material. The *Spin-Zone* associated with surface S_1 is identified and a toolpath corresponding to boundary of the *Spin-Zone* is labeled **F**. The second point of contact lies on surface S_2 and is labeled as **F'**. There are two possible solutions for **F'** and they correspond to whether the tool is rotated in clockwise direction or in the counter clockwise direction. The trajectory of the second point of contact wander and depends on the properties of surface S_2.

To ensure that all the unwanted material is machined, the *Spin-Zone* due to drop surface S_2 is determined. This is shown in Figure 5(b). It must be noted that the snugly tool position is identical in both cases as shown in Figures 5(a) and 5(b). A toolpath corresponding to the edge of the spin zone is identified and labeled as **E**. The two points of contact can be seen in Figure 5(b). The two sets of tool paths shown in Figure 5(a) and Figure 5(b) do not cover the same area of surfaces S_1 and S_2. Thus, to ensure the coverage of the largest amount of area ensconced within the spin zones due to surface $S_1$and S_2, the two sets of toolpaths are combined.

Similar results for multi-pass finish machining of common edge region between two intersecting bi-quadratic convex Bézier surfaces are shown in Figure 6(a) and 6(b).

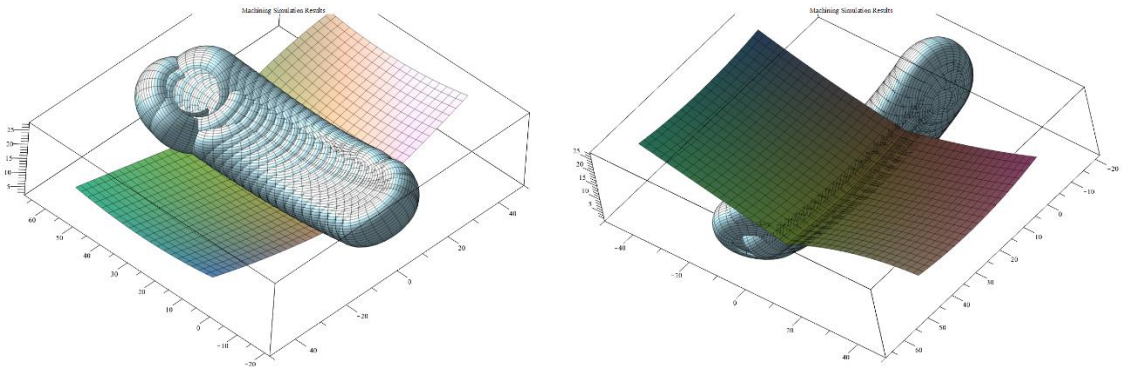

(a) (b)

Figure 7: Simulation of multi-pass tool paths for finish machining of common edge between two intersecting Bi-quadratic concave surfaces: (a) Top view ($\boldsymbol{S_1}$ towards left, $\boldsymbol{S_2}$ towards right), (b) Bottom view ($\boldsymbol{S_1}$ towards left, $\boldsymbol{S_2}$ towards right).

DSM multi-pass toolpaths for finish machining of the common edge between the test surfaces are also simulated in Maple™ for validation by plotting the surfaces and the tool orientations

© 2020 CAD Solutions, LLC, http://www.cad-journal.net

corresponding to all tool drop locations as shown in Figures 7 and 8. Top and bottom views clearly show that all tool positions in the multi pass tool paths are gouge free.

In addition to graphical verification of the five-axis toolpath data, we also tested the concept by actual machining of the pairs of concave and convex surfaces on aluminum alloy specimens on a DMU-80P Hi-Dyn tilt-rotary simultaneous five-axis machining center. In this paper, we are presenting the results for machined convex surfaces and are shown in Figure 9. The tool geometry used for the actual machining has insert radius $R_i = 6mm$ and offset radius $R_o = 6.7mm$. The rough machining of aluminum blocks of size $100mm \times 50mm \times 40mm$ is carried out using five-axis tool paths generated by Drop and Tilt Method (DTM) using triangulated approximation of the composite surfaces [5]. Alternatively, the rough machining of work specimen can also be done by any other 3 axis or 5-axis machining technique. Rough machined specimens have substantial amount of uncut material in the common edge region due to limited accessibility of the toroidal tool using DTM tool positioning. This can be seen by comparing Figures 9(a) and 9(d). The surface after machining the snuggly fit pass as a radiused transition surface is seen as a narrow strip along the common edge in Figure 9(b). The snugly fit pass corresponds to trajectory **A** shown in Figure 6 for pair of convex surfaces. The surface resulting after additional tool passes (corresponding to trajectories **B** to **F** in Figure 6(b)) due to surface S_2 is shown in Figure 9(c). These passes remove additional material on one side of the common edge. Subsequently, another set of additional tool passes (corresponding to trajectories **B** to **F** in Figure 6 (a)) due to surface S_1 remove excess material on the other side of the common edge as shown in Figure 9(d). The accuracy of the machined snug pass was tested on a coordinate measuring machine at two locations and was found to be within 30 microns of the simulated results [13].

It is clear that additional tool passes are required to remove material across the common edge. Using addition tool paths based on *Spin-Zone* associated with surface S_2 is not enough to remove all the material. Combining the tool paths based on the *Spin-Zone* associated with S_1 and S_2 is required to machine all the unwanted material.

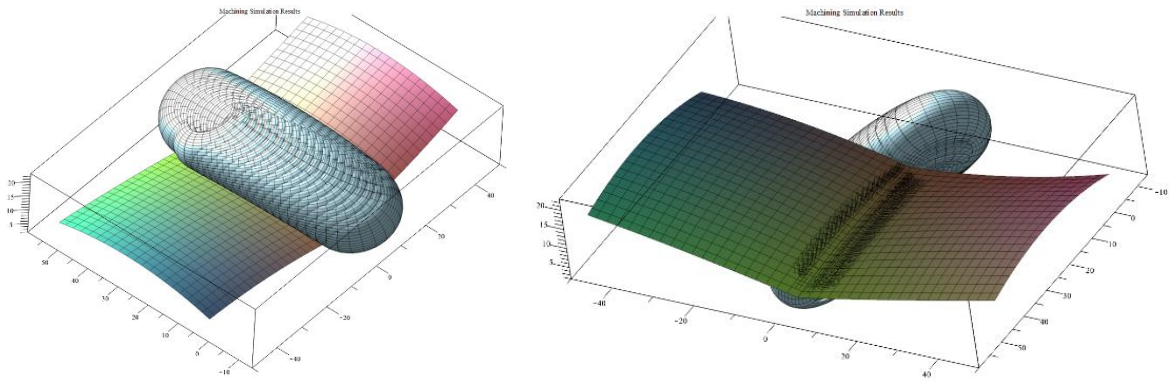

(a) (b)

Figure 8: Simulation of multi-pass tool paths for finish machining of common edge between two intersecting Bi-quadratic convex surfaces: (a) Top view (S_1 towards left, S_2 towards right), (b) Bottom view (S_1 towards left, S_2 towards right).

© 2020 CAD Solutions, LLC, http://www.cad-journal.net

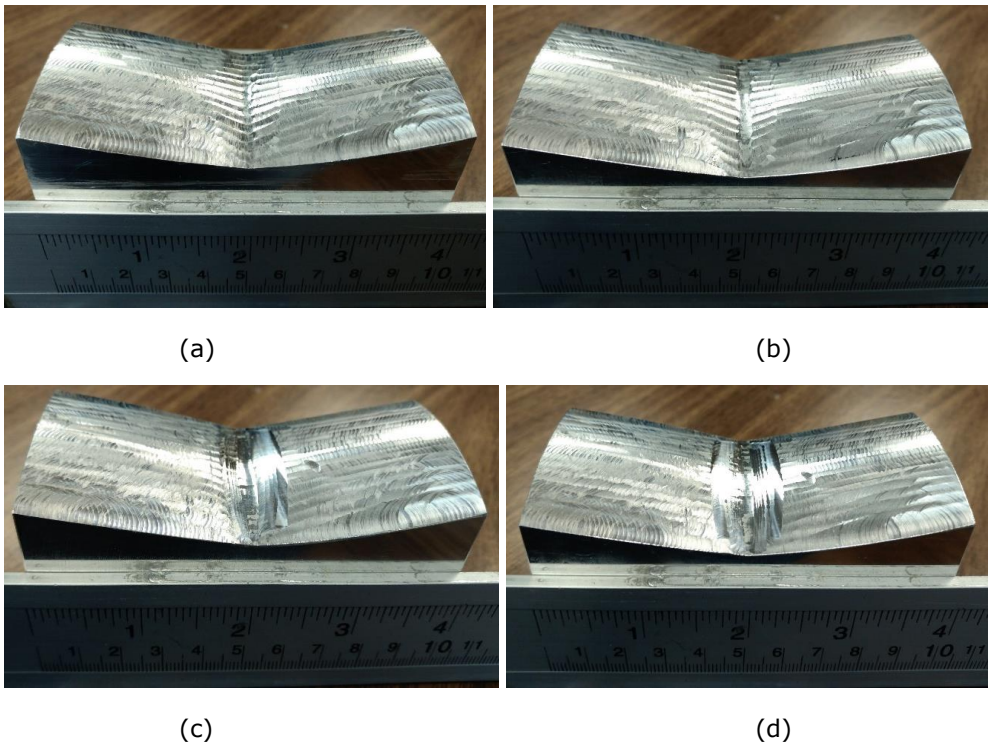

(a) (b)

(c) (d)

Figure 9: Set of Bi-quadratic convex Bézier surfaces (S_1 towards left and S_2 towards right in all figures) machined on DMU-80P-Hi-Dyn tilt-rotary simultaneous 5-axis machining center: (a) Surfaces rough machined with DTM, (b) radiused corner formed in the common edge region after snugly fit machining pass, (c) Machined surfaces after implementing additional cleanup passes using toolpaths due to tool-drop surface S_2, (d) Machined surfaces after implementing additional cleanup passes using toolpaths due to tool-drop surface S_1.

5 CONCLUDING REMARKS

Multipoint five-axis machining of an intersection edge of a composite surface patch is investigated in this work. A number of techniques can be employed for machining the composite surface patches, but five-axis machining using toolpath data generated by DSM approach for a toroidal end mill near the common edge region is found to be an effective method. DSM provides a smooth toolpath to finish machine the common edge zone. The snugly fit DSM machining pass creates a radiused transition surface but leaves unwanted material between the snuggly fit pass and the boundary of the *Spin-Zones* on either surface. Additional five-axis tool passes created by dropping the tool in the *Spin-Zone* due to tool-drop surface S_1 are not enough to completely remove all the unwanted material in the common edge region. Tool passes created by dropping tool in the spin zone of surface S_2 are necessarily required to remove all the unwanted material. Though, the spacing between the two contact points on the intersecting surfaces can be controlled by selecting the appropriate tool drop footprint within the *Spin-Zone* limits, but this gap between contact points is also dependent on the geometry of the toroidal tool and its size. The radius of the pseudo insert circle R_i dictates the radius of common edge in snuggly fit pass. So common edges with smaller radii can be machined by selecting the toroidal tool with suitable insert radius subject to kinematic constraints of the machine. It is observed in this work that for each tool drop position within the *Spin-Zone*, there are two possible solutions for second point of contact on the spin-surface leading to two possible five-

© 2020 CAD Solutions, LLC, http://www.cad-journal.net

axis tool positioning solutions. One of the tool orientation leads to removing un-machined material using the leading edge of the tool while the other removes material using the trailing edge. A considerate choice out of the leading edge or trailing edge tool positioning solution can ensure a good surface finish in fewer five-axis machining passes.

6 ACKNOWLEDGEMENTS

This research is supported by five-axis machining group at University of Waterloo, Canada and is funded by the Natural Sciences and Engineering Research Council of Canada.

Sandeep Kumar Sharma, https://orcid.org/0000-0003-2469-2825
Ravinder Kumar Duvedi, https://orcid.org/ 0000-0001-6696-9779
Sanjeev Bedi, https://orcid.org/0000-0002-6993-8502
Stephen Mann https://orcid.org/0000-0001-8528-2921

7 REFERENCES

[1] Bedi, S.; Gravelle, S.; Chen, Y.: Principal curvature alignment technique for machining complex surfaces, Journal of manufacturing science and engineering, 119(4B), 1997, 756-765. http://manufacturingscience.asmedigitalcollection.asme.org/article.aspx?articleid=1433682

[2] Bedi, S.; Ismail, F.; Mahjoob, M. J.; Chen, Y.: Toroidal versus ball nose and flat bottom end mills, International Journal of Advanced Manufacturing Technology, 13(5), 1997, 326–332. https://doi.org/10.1007/BF01178252

[3] Chen, Z.; Li, S.; Gan, Z.; Zhu, Y.: A highly efficient and convergent optimization method for multipoint tool orientation in five-axis machining, International Journal of Advanced Manufacturing Technology, 93, 2017, 2711–2722. https://doi.org/10.1007/s00170-017-0688-0

[4] Duvedi R. K.; Bedi S.; Mann S.: An efficient multipoint 5-axis tool positioning method for tensor product surfaces, International Journal of Advanced Manufacturing Technology, 97, 2018, 279–295. https://doi.org/10.1007/s00170-018-1940-y

[5] Duvedi, R. K.; Bedi, S.; Batish, A.; Mann, S.: A multipoint method for 5-axis machining of triangulated surface models, Computer-Aided Design, 52, 2014, 17–26. https://dx.doi.org/10.1016/j.cad.2014.02.008

[6] Duvedi, R. K.; Bedi, S.; Mann, S.: Numerical implementation of drop and tilt method of 5-axis tool positioning for tensor product surfaces, International Journal of Advanced Manufacturing Technology, 95, 2018, 219–232. https://doi.org/10.1007/s00170-017-1193-1

[7] Gray, P.; Bedi, S.; Ismail, F.: Arc-intersect method for 5-axis tool positioning, Computer-Aided Design, Elsevier, 37, 2005, 663-674. https://doi.org/10.1016/j.cad.2004.08.006

[8] Gray, P.; Ismail, F.; Bedi, S.: Graphics-assisted rolling ball method for 5-axis surface machining, Computer-Aided Design, Elsevier, 36, 2004, 653-663. https://doi.org/10.1016/S0010-4485(03)00141-6

[9] He, Y.; Chen, Z.: Optimizing tool positioning for achieving multi-point contact based on symmetrical error distribution curve in sculptured surface machining, International Journal of Advanced Manufacturing Technology, 73(4), 2014, 707–714. https://link.springer.com/article/10.1007%2Fs00170-014-5862-z

[10] Lasemi, A.; Xue, D.; Gu, P.: Recent development in CNC machining of freeform surfaces: A state-of-the-art review, Computer-Aided Design, 42, 2010, 641–654. https://doi.org/10.1016/j.cad.2010.04.002

[11] Rao, N.; Ismail, F.; Bedi, S: Tool path planning for five-axis machining using the principal axis method, International Journal of Machine Tools Manufacture, 37(7), 1997, 1025–1040. https://doi.org/10.1016/S0890-6955(96)00046-6

© 2020 CAD Solutions, LLC, http://www.cad-journal.net

[12] Sharma, S. K.; Duvedi, R. K.; Bedi, S.; Mann, S.: A method for generating multiple solutions for multipoint five-axis tool positioning, International Journal of Advanced Manufacturing Technology, published online Oct 2018. https://doi.org/10.1007/s00170-018-2871-3
[13] Sharma, S. K.; Duvedi, R. K.; Bedi, S.; Mann, S.: A multipoint tool positioning method for five-axis machining in the region of two intersecting tensor product Bézier surfaces, Accepted for publication Journal of Machine Tool and Manufacture in April 2019. https://doi.org/10.1016/j.ijmachtools.2019.04.007
[14] Wang, G.; Li, W. L.; Rao, F.; He, Z. R.; Yin, Z. P.: Multi-parameter optimization of machining impeller surface based on the on-machine measuring technique, Chinese Journal of Aeronautics, October 2018. https://doi.org/10.1016/j.cja.2018.09.005
[15] Warkentin, A.; Ismail, F.; Bedi, S.: Comparison between multipoint and other 5-axis tool positioning strategies, International Journal of Machine Tools Manufacture, 40(2), 2000, 185–208. https://pdfs.semanticscholar.org/f51f/6a8982469e8614ed7895d73b2ad49edc84f1.pdf
[16] Warkentin, A.; Ismail, F.; Bedi, S.: Intersection approach to multi-point machining of sculptured surfaces, Computer Aided Geometric Design, 15, 1998, 567-584. https://doi.org/10.1016/S0167-8396(97)00039-3
[17] Warkentin, A.; Ismail, F.; Bedi, S.: Multipoint tool positioning strategy for 5-axis machining of sculptured surfaces, Computer Aided Geometric Design, 17(1), 2000, 83-100. https://doi.org/10.1016/S0167-8396(99)00040-0
[18] Wu, B.; Liang, M.; Zhang, Y.; Luo, M.; Tang, K.: Optimization of machining strip width using effective cutting shape of flat-end cutter for five-axis free-form surface machining, International Journal of Advanced Manufacturing Technology, 94, 2017, 2623–2633. https://doi.org/10.1007/s00170-017-0953-2

© 2020 CAD Solutions, LLC, http://www.cad-journal.net